

# Restoration and Enhancement of Underwater Under-Exposure Images with Detail-Preserving

Xujian Li

shandong university of science and technology

Ke Liu (✉ [keliucs@163.com](mailto:keliucs@163.com))

Shandong University of science and technology

---

## Research

**Keywords:** Edge detail enhancement, guided filter, underwater under-exposure images

**Posted Date:** February 27th, 2020

**DOI:** <https://doi.org/10.21203/rs.2.24728/v1>

**License:**   This work is licensed under a Creative Commons Attribution 4.0 International License.

[Read Full License](#)

---

# 1 Restoration and Enhancement of Underwater 2 Under-Exposure Images with Detail-Preserving

3 Xujian Li <sup>1</sup>, Ke Liu <sup>2\*</sup>

4 <sup>1</sup> Shandong university of science and technology

5 <sup>2</sup> Shandong university of science and technology

6 Received: date; Accepted: date; Published: date

7 **Abstract:** Underwater images have great practical value in many fields such as underwater  
8 archeology, seabed mining, and underwater exploration. Due to the complex underwater  
9 environment, there are problems such as poor light, low contrast, and color degradation.  
10 Traditional underwater image processing methods cannot well achieve the goal of clear display  
11 under extreme conditions. This paper proposes a method for restoration and enhancement of  
12 underwater under-exposure images that protects edge details and enhances image color. Firstly,  
13 the underwater image was preprocessed, denoising with improved wavelet threshold function,  
14 defogging with the Multi-Scale Retinex Color Restoration (MSRCR) and guided filter method.  
15 Then, the method of adaptive exposure graph is used to enhance the under-exposure image.  
16 Finally, the deep learning algorithm combined with the Non-Subsampled Contour Transform  
17 (NSCT) technology is used to solve the problem of color degradation and edge texture weakening.  
18 Experiments show that compared with other underwater image processing methods, this method  
19 greatly improves the clarity of the image, enhances the color saturation and the edge texture details  
20 of the image, and has a better visual effect.

21 **Keywords:** Edge detail enhancement; guided filter; underwater under-exposure images

---

## 23 1. Introduction

24 At present, more and more activities are carried out underwater by human beings, such as  
25 underwater archaeology, seabed biological collection, Marine fishery breeding and so on. Due to the  
26 complicated underwater environment, the obtained images often appear dim, noisy, color  
27 degradation, detail loss and other problems, there is an urgent need for clear, high-quality  
28 underwater images.

### 29 1.1. Research status and problems

30 For these problems, [1] proposed a weighted mapping for each image based on some  
31 established exposure metrics, then an orderly fusion is performed. During the fusion process, each  
32 image must have different exposure information. However, this solution does not take into account  
33 the movement of the camera during the image exposure. Therefore, caused image blur; In response  
34 to this situation, [2] proposed a method using only a single under-exposure underwater image.  
35 Firstly, an LDR image was generated from a histogram. Next, the high-frequency region of the LDR  
36 image obtained in the foregoing is combined with the smooth region of the average filtered image to  
37 jointly denoise. Finally, the LDR image is fused to generate a new image. In the image fusion  
38 operation, although the edge details of the image are retained, the intensity of the image is reduced,  
39 and the color of the image is degraded, that is, the color of the image is enhanced And retaining the  
40 details is not the best of both worlds, many image fusion methods also have such problems; Some  
41 people use energy as the minimum value to obtain the best results. Reference[3] uses the energy  
42 function composed of two terms to achieve the effect of enhancing the exposed image, although it  
43 can retain the image color and edge texture However, it is necessary to increase the smoothness  
44 constraint on the image, so that the computational complexity of the image is greatly increased, and  
45 the generation efficiency is reduced; Literature [4] proposed a realization idea of the red channel.

46 Experiments have shown that although the color related to short wavelength can be enhanced, the  
47 method used is limited by the accuracy of the optical model and parameter estimation; Reference[5]  
48 proposed a Rayleigh-distributed color model fusion method, which not only reduced image noise,  
49 but also improved the contrast of the image to a certain extent, but led to excessive image  
50 enhancement; The enhancement method of underwater image based on defogging and color  
51 correction proposed in [6], although it solves the interference of noise and fog, however, there may  
52 also be problems with insufficient or excessive image enhancement; Reference [7] used a single  
53 underwater image restoration method by combining the blue-green channel and the red channel.  
54 First, the blue-green channel was restored by the defogging algorithm, and then the red channel was  
55 corrected by using the gray world hypothesis theory. Adapting to the exposed image and solving  
56 the problems of overexposure and underexposure largely eliminated the exposure problem of the  
57 image, but did not retain the details of the image well; Reference [8] proposed an under-exposure  
58 image enhancement method that achieves detail preservation through optimal weighted multiple  
59 exposure fusion. First, a multiple exposure image sequence is generated, and then an energy  
60 function is constructed to preserve the image color and edge detail parts. The method eliminates the  
61 exposure, retains the color of the image well, and the image enhancement effect is obvious, but the  
62 poor coloring and noise still exist in the dark area, and the calculation efficiency of the algorithm is  
63 not high.

## 64 1.2. The work of this paper

65 For the above-mentioned series of problems, this paper implements a method for restoration  
66 and enhancement of underwater underexposure images with preserved details. Firstly, the  
67 improved wavelet denoising function was used to remove a series of noises in the image, and the  
68 Multi-Scale Retinex with Color Restoration (MSRCR) was combined with the guided filter to solve  
69 the problem of fog in the underwater image. Because of the combination of the guided filter, it also  
70 protects the edge details, which greatly improves the image quality. Then, for the problem of low  
71 light in the image, an improved image histogram equalization method is adopted in this paper,  
72 which not only improves the brightness of the image, but also preserves and enhances the color of  
73 the image. The method of adaptive exposure combined with guided filter uses the optimal adaptive  
74 exposure map, so that the problem of uneven lighting is well solved, and the algorithm  
75 implementation is very efficient; Finally, for the underwater image after adaptive exposure  
76 processing, the color degradation of some areas may exist. This paper uses super-resolution  
77 convolutional neural network (SRCNN) combined with non-subsampled contour transform (NSCT)  
78 method, which is effective to enhances the color of underwater images, and also solves the problem  
79 of local edge texture loss. The experiments in the real image library show that compared with other  
80 methods, the MSRCR combined with the guided filter defogging method, the exposure image  
81 enhancement method, and SRCNN combined with the NSCT method are used in defogging,  
82 denoising, detail preservation and exposure enhancement Even better. The main contributions of  
83 this paper are as follows:

- 84 • A new method for defogging underwater under-exposure images is proposed, which is better  
85 than the latest method for defogging and keeps edge details.
- 86 • The super-resolution convolutional neural network is combined with the guided filter, which  
87 can enhance the color and protect the edge details of the image after adaptive exposure processing.  
88 As a result, the quality and clarity of the image is better.
- 89 • The algorithm implemented in this paper is simple and the computational efficiency is higher  
90 than other methods.

91 The structure of this paper is as follows: the first part briefly introduces the research method  
92 and algorithm of this paper. The second part introduces the method of image restoration. The third  
93 part introduces the image enhancement method. The fourth part is the experimental results and  
94 analysis of this method. Finally, the conclusion is given.

## 95 2. Related Work

96 The processing of underwater images is mainly focused on the dehazing, denoising, and  
 97 enhancement of color and edge details. We discuss the background of the related works in the  
 98 following sections.

## 99 2.1. Wavelet threshold function

100 The denoising effect of the traditional wavelet threshold function is related to the threshold  
 101 function and reconstruction accuracy, while the traditional threshold function mainly includes soft  
 102 threshold and hard threshold functions.

103 Where the hard threshold function is expressed as:

$$104 s_{j,k} = \begin{cases} \rho_{j,k} & |\rho_{j,k}| > \delta \\ 0 & |\rho_{j,k}| \leq \delta \end{cases} \quad (1)$$

105  $\rho_{j,k}$  Represents the wavelet coefficient with noise,  $s_{j,k}$  Represents the output wavelet  
 106 coefficient. When the hard threshold function is used, it will protect some details, but the function is  
 107 discontinuous at the  $\pm\delta$ . Therefore, in the process of reconstruction of wavelet coefficients,  
 108 Gibbs-like phenomena is easy to occur.

109 Soft threshold function:

$$110 s_{j,k} = \begin{cases} \text{sgn}(\rho_{j,k}) * (\rho_{j,k} - \delta) & |\rho_{j,k}| > \delta \\ 0 & |\rho_{j,k}| \leq \delta \end{cases} \quad (2)$$

111 Formula (2) can be concluded that the soft threshold function improves the flaw of the hard  
 112 threshold function, that is, the soft threshold function is continuous at  $\pm\delta$ , but will lead to the loss of  
 113 local value.

## 114 2.2. Super-resolution convolutional neural network (SRCNN)

115 The task goal of super resolution is to convert the input low-resolution image into  
 116 high-resolution image, which is consistent with image de-noising and image de-blurring.  
 117 Super-resolution focuses on how images from small to large sizes are filled with new pixels; Image  
 118 de-noising is concerned with replacing the "contaminated" pixels with the correct ones without  
 119 changing the image size.

120 SRCNN is the first end-to-end super-resolution algorithm using CNN architecture (that is,  
 121 based on deep learning), which is better than the traditional multi-module integration method.

122 1)The structure of SRCNN is relatively simple. The whole convolutional network consists of  
 123 three convolutional layers, even without pooling and full connection layers;

124 2) Convolution operation is performed on low-resolution graphs to generate n1-dimensional  
 125 feature maps;

126 3) Conduct convolution operation on n1-dimensional feature map to generate n2 dimensional  
 127 feature maps;

128 4) The n2 dimension feature maps are convolved to generate super-resolved images.

129 There are three processing processes:

130 1) Extract image features: extract multiple patch image blocks from low-resolution images. Each  
 131 block is represented by convolution operation as a multi-dimensional vector (the dimension is equal  
 132 to the number of filters), and all feature vectors constitute feature maps.

133 2) Nonlinear mapping: the n1 dimensional feature matrix is transformed into another n2  
 134 dimensional feature matrix through convolution operation to realize the nonlinear mapping.

135 3) Image reconstruction: it is equivalent to a deconvolution process, and the characteristic  
 136 matrix of n2 is restored to the super-resolved image.

137 The objective loss of the training is to minimize the super-resolution image and the original  
 138 high-resolution image X based on pixel mean square error. The definition is as follows:

$$139 L(\theta) = 1/n \sum_{i=1}^n \|F(Y_i; \theta) - X_i\|^2 \quad (3)$$

140 Where, n is the number of training samples, that is, the number of samples for each training.  
 141 The next step is nothing more than the stochastic gradient descent method back propagation,  
 142 network training to obtain the final parameter to minimize the loss , the parameter update formula is  
 143 as follows:

$$144 \quad \Delta_{i+1} = 0.9 * \Delta_i + \mu(\partial L / \partial W_i^\delta) \quad (4)$$

$$145 \quad W_{i+1}^\delta = W_i^\delta + \Delta_{i+1} \quad (5)$$

### 146 2.3. Multi-scale retinex with color restoration (MSRCR)

147 Retinex is a combination of the words Retina and Cortex. Retinex theory mainly includes two  
148 aspects: the color of an object is determined by its ability to reflect long, medium and short waves,  
149 rather than by the absolute value of the intensity of the reflected light; The color of the object is not  
150 affected by the inhomogeneity of illumination and has consistency.

151 Single Scale Retinex, with a small Scale value, can better complete the dynamic range  
152 compression, and the details of the dark region can be better enhanced, but the output color is prone  
153 to distortion. When the value is larger, the color sense consistency is better.

154 Multi-scale Retinex can not only realize the compression of dynamic range of images, but also  
155 keep the consistency of color perception. The implementation steps are slightly different than those  
156 of a single scale, but both have problems with color skew. Multi-scale Retinex with Color Restoration  
157 (MSRCR) for better visual effects. In comparison, (1) the effect of MSRCR is much better than that of  
158 MSR, basically eliminating color bias. (2) for MSRCR, the resulting image of scale number pair is not  
159 particularly large, but the algorithm time will increase linearly with the increase of scale number.  
160 Therefore, it is more appropriate to take 3 as the general scale number.

### 161 2.4. Non-subsampled contour transform (NSCT)

162 The core of the Non-Subsampled Contour Transform (NSCT) transformation is Contourlet, the  
163 transformation of the edge. Non-downsampling is based on the frequency domain, that is, for an  
164 image, a frequency threshold is set first, and then the image is screened out with a filter that is greater  
165 than or equal to the threshold frequency (of course, this is not a one-time screening process, but an  
166 iterative process of using a two-channel bandpass filter without downsampling).

## 167 3. Methodology

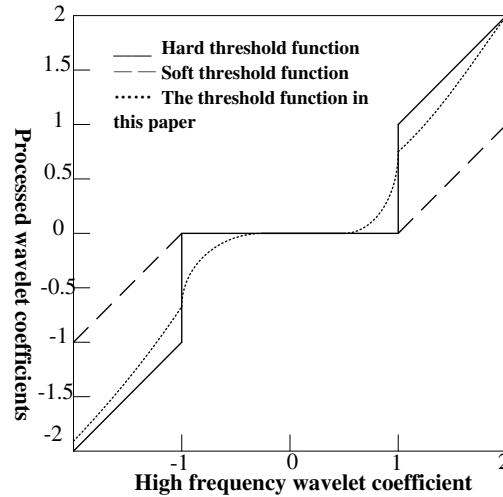
168 Due to the uneven distribution of underwater light, the water body contains many impurities,  
169 and the uncertainty of the external environment at the time of shooting the images, the images  
170 obtained under water contain different levels of noise and underwater fog. In this paper, an  
171 improved wavelet threshold function is used to denoise, and a combination of MSRCR and a guided  
172 filter is used to remove underwater fog. Experiments prove that the methods of de-drying and  
173 defogging adopted in this paper are better than the current optimal methods.

### 174 3.1. Image Denoising

175 In order to further make up for the shortcomings in the two functions, this article has made  
176 improvements. By transforming the base value of the exponential function and the independent  
177 variable, the wavelet coefficients can be further manipulated to better solve the noise problem. And  
178 the function is uninterrupted at  $|\rho_{j,k}| = \delta$ , perfecting the shortcomings of the hard threshold and  
179 soft threshold functions, the formula is as follows:

$$180 \quad s_{j,k} = \begin{cases} 1 + \operatorname{sgn}(\rho_{j,k}) * \left[ \rho_{j,k} - \frac{\delta}{2+\alpha} * \mu \sqrt[3]{\rho_{j,k}^2 - \delta^2} \right] & |\rho_{j,k}| > \delta \\ 1 + \operatorname{sgn}(\rho_{j,k}) * \frac{\alpha}{2+\alpha} * b^{10 * (|\rho_{j,k}| - \delta)} * |\rho_{j,k}| & |\rho_{j,k}| \leq \delta \end{cases} \quad (6)$$

181  $\rho_{j,k}$  Represents the wavelet coefficient with noise,  $s_{j,k}$  Represents the output wavelet  
182 coefficient,  $\delta$  and  $\alpha$  are two parameters. This function performs better in denoising images  
183 than other denoising functions, and computes more efficiently. Fig.1 shows the comparison of the  
184 three functions.



185

186

Fig.1.Comparison of different threshold function curves

187

The curve comparison chart of the hard threshold function, soft threshold function and the threshold function used in this paper is shown in Figure 1. Comprehensive analysis shows that the threshold function in this paper is better than the hard and soft threshold functions in processing.

189

190

In formula (6), the selection of the threshold value  $\delta$  has a great influence on the de noising. If  $\delta$  is selected too small, the noise will not be completely removed, resulting in unsatisfactory image effects; if  $\delta$  is too large, the denoising Excessive, resulting in distortion of the image. Therefore, this paper uses the method of Bayesian threshold [9] to make the threshold of each layer automatically shrink as the wavelet decomposition scale increases:

192

193

194

$$z(X) = E(\tilde{x} - x)^2 = E_x E_{x|y}(\tilde{x} - x)^2 = \iint (n(y) - x)^2 P(y|x) P(x) dy dx = \gamma^2 \rho\left(\frac{\gamma^2}{\gamma_x^2}, X/\gamma\right) \quad (7)$$

195

$$\rho(\gamma_x^2, X) = \gamma_x^2 + 2(X^2 + 1 - \gamma_x^2) \varphi\left(\frac{X}{\sqrt{1+\gamma_x^2}}\right) - 2X(1 + \gamma_x^2) * \varphi(X, 1 + \gamma_x^2) \quad (8)$$

196

197

Density function:

198

$$\varphi(x, \gamma_x^2) = (1/\sqrt{2\pi\gamma^2}) e^{(-x^2/2\gamma^2)} \quad (9)$$

199

$$\overline{\varphi(x)} = \int_x^\infty \varphi(t, 1) dt \quad (10)$$

200

Threshold calculation expression:

201

$$X_j = \gamma^2/\gamma_x \quad (11)$$

202

Among them,  $\gamma^2$  represents the variance of noise,  $\gamma_x$  represents the standard deviation of the sub-band coefficients, and j represents a certain layer of the layer.

203

For the calculation of  $\gamma^2$  in (11), the method mentioned in [9] is used:

204

$$\gamma = \text{median}(|s_{j,k}|)/0.6745 \quad (12)$$

205

$$\overline{\gamma} = 1/n \sum_{i=1}^n s_{j,k}^2 \quad (13)$$

206

In formula (13), n represents the length of the decomposition wavelet coefficient of each layer, which is known from  $\gamma_s^2 = \gamma^2 + \gamma_x^2$ :

207

$$\gamma^2 = \sqrt{\max(\gamma_s^2 - \gamma_x^2, 0)} \quad (14)$$

208

Therefore, according to (12) (13) (14), the Bayesian threshold is jointly obtained, that is, the adaptiveness of the Bayesian threshold between different layers is obtained, thereby highlighting the benefits of the algorithm in this paper.

209

For the parameters  $\delta$  and  $\alpha$  in the improved threshold function, this paper uses the particle swarm optimization algorithm mentioned in [10] to solve.

210

By applying the improved wavelet threshold function to the de-noising problem of underwater images, a series of noises appearing in the image are fully solved, and the visual effect of the image is greatly improved. The de-noising effect is shown in Fig.2.

211

212

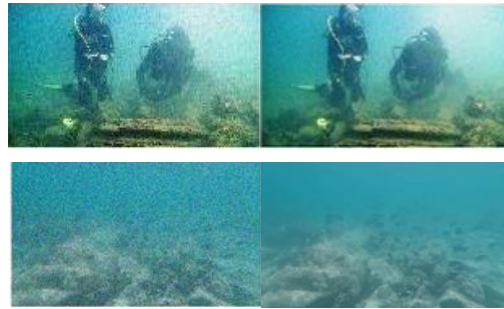
213

214

215

216

217



(a) Original image (b) Denoised image

**Fig.2.** Denoising results

218

219

220

221

### 222 3.2. Image defogging

223 In order to overcome the problem of the color deviation of Multi-Scale Retinex(MSR) and the  
 224 image enhancement effect is not ideal, reference [11] used the MSRCR algorithm to deal with the  
 225 problem of image enhancement. Although the effect of MSR color shift was largely eliminated, the  
 226 image still has the problem of faded details. Aiming at such problems, this paper proposes a  
 227 method of combining the MSRCR algorithm with a guided filter to complete the defogging of  
 228 underwater images.

$$229 \text{RMSRCR}(x, y)' = G \cdot \text{RMSRCR}(x, y) + b \quad (15)$$

$$230 \text{RMSRCR}(x, y) = C(x, y)\text{RMSR}(x, y) \quad (16)$$

$$231 C(x, y) = f\left[\frac{I'(x, y)}{\sum I(x, y)}\right] C_i(x, y) = f[I'_i(x, y)] = f[I_i(x, y) \sum j] \quad (17)$$

$$232 f[I'(x, y)] = \beta \log[\alpha I'(x, y)] = \beta \{\log[\alpha I'(x, y)] - \log[\sum I(x, y)]\} \quad (18)$$

233 Among them,  $G$  represents the gain Gain (usually 5),  $b$  represents the offset Offset (usually  
 234 25),  $I(x, y)$  represents the image of a channel,  $C$  represents the color recovery factor of a channel,  
 235 adjust the ratio of the color of the three channels,  $f(*)$  represents the mapping relationship of the  
 236 color space,  $\beta$  refers to the gain constant (valued as 46), and  $\alpha$  refers to the controlled non-linear  
 237 intensity (valued as 125).

238 Experiments prove that MSRCR can remove the fog phenomenon in the original underwater  
 239 image well, and enhance the contrast and saturation of the color in the image. The guide filter can  
 240 protect the edge details and also has a certain defogging function. The combination of the two  
 241 methods not only makes the defogging effect more efficient, but also enhances the color of the  
 242 image to a certain extent and the edge details more clearly, thereby improving the efficiency of the  
 243 algorithm. Fig.3 is an image result of continuing the defogging based on Fig.2. It is obvious from  
 244 figure 3 that the de-fogging method adopted in this paper has a very ideal de-fogging effect.



(the original image on the left; the image after the dehazing on the right)

**Fig.3.**Dehazing effect

245

246

247

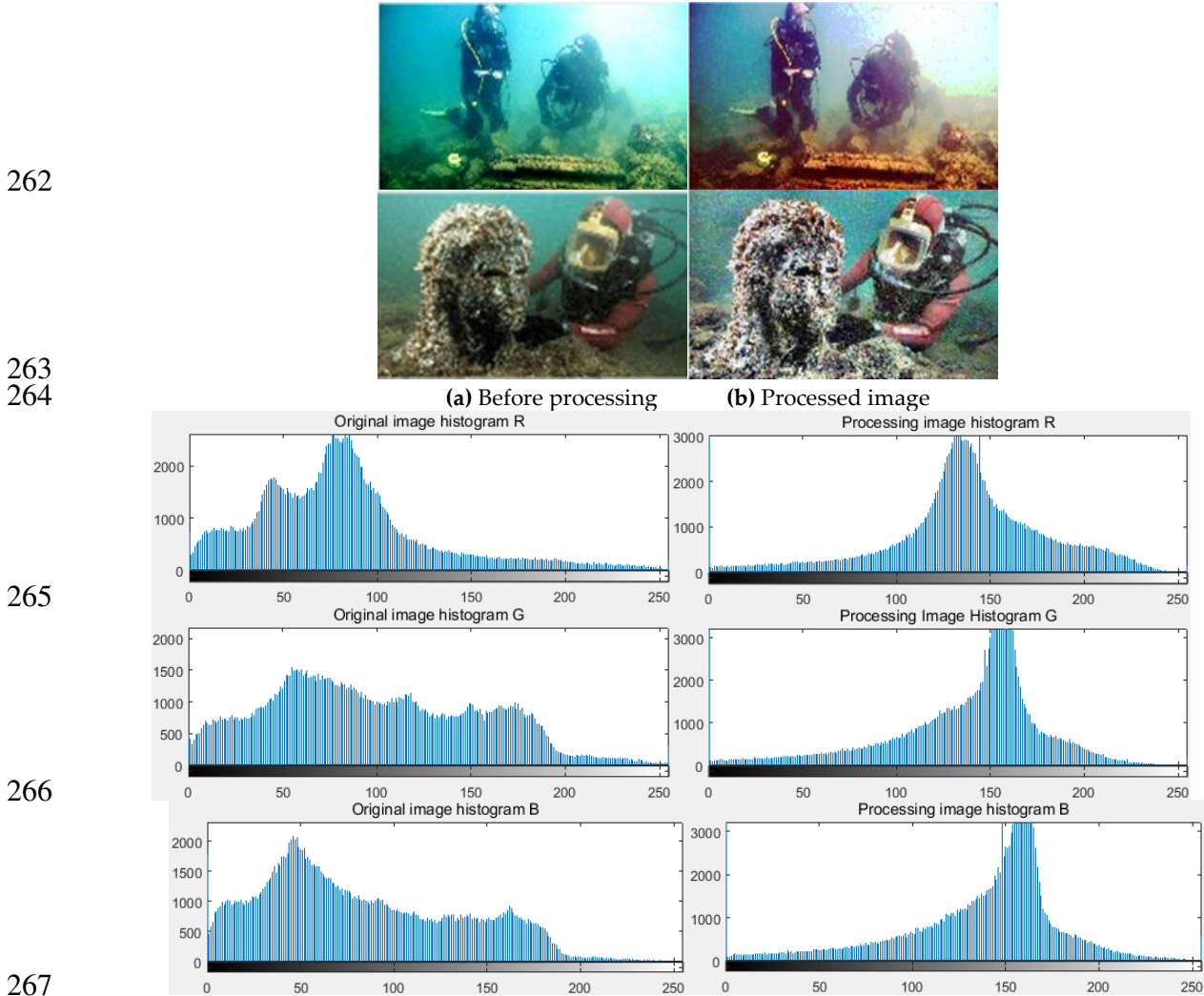
248

### 249 3.3. Underwater image enhancement

250 For underwater archaeology and Marine biological collection, it is difficult to obtain clear  
 251 underwater images due to the change of underwater water flow, uneven lighting and other

252 practical conditions, but the practical value is becoming higher and higher. Therefore, it is very  
 253 important to enhance the underwater under-exposure image.

254 After the previous image restoration stage, to some extent, some information can be obtained  
 255 from the current image, but there is still the problem of low image brightness. In response to this  
 256 problem, this paper uses the improved histogram equalization image enhancement method  
 257 proposed by Dong Lili et al. [12] to process the image, which has two effects:1) Improved the  
 258 bright- ness of underwater under-exposure images;2) It also has a great effect of maintaining and  
 259 enhancing the color of the image, avoiding the appearance of Artefact. However, experiments have  
 260 shown that in the process of increasing the brightness of this method, some images may cause some  
 261 areas of the resulting image to appear lighter or darker. See Figure 4.



267  
 268  
 269 **Fig.4.** Improved histogram equalization results

270 In view of the above phenomena, this paper uses an adaptive exposure map method. First, we  
 271 further improved the adjustment results based on the adaptive exposure map [13], and obtained the  
 272 adaptive image exposure map  $f(x)$  from the solution of the optimal value in this document:

$$273 \min_f \sum_x \{ [2 - f(x)Y_{f(x)}/Y_{I(x)}]^2 + \alpha[f(x) - 2]^2 \} + \varphi(f) \quad (19)$$

274 Among them,  $f(x)$  represents the adaptive risk map,  $Y_{f(x)}$  represents the light intensity of the  
 275 restored image,  $Y_{I(x)}$  represents the light intensity of the input image,  $\alpha$  is a constant 0.3, and  $\varphi(*)$   
 276 represents a smooth positive Regularization.

277 The optimization solution is divided into two steps. The first is to solve  $f(x)$  when  $\varphi(*)$  is  
 278 ignored, which is an auto-closed value; the second is to introduce the guided filter into the solution,  
 279 which leads to the ideal answer. Here, the estimation function is obtained as:

$$f(x) = GF_I[(Y_{J(x)}Y_{I(x)} + \alpha Y_{I(x)}^2)/(Y_{J(x)}^2 + \alpha Y_{I(x)}^2)] \quad (20)$$

281 Further draws:

$$282 \text{ OutputExp} = J^c(x) * f(x), c \in \{r, g, b\} \quad (21)$$

283 Among them,  $J^c(x)$  represents a restored image, and  $f(x)$  represents an adaptive exposure  
284 image.

285 Under-exposure images, the processed images have the problem of edge detail dilution to  
286 varying degrees, accompanied by the occurrence of local edge color degradation. To this end, the  
287 improved super-resolution convolutional neural network (SRCNN) combined with the non-sub  
288 sampled contour transform (NSCT) technology is used to enhance the image color and edge details.  
289 Based on the super-resolution based on color features proposed in reference [14-15], this paper  
290 makes some improvements. Firstly, the initial image is optimized by SRCNN, which contains three  
291 convolutional neural layers. The original image is divided into three parts, namely RGB channel.  
292 Then, using CNN to perform training operation on the image, three new images are obtained, and  
293 the new images are fused with each other to obtain the fused image. Finally, the fused image is  
294 processed by NSCT [16-17] to obtain the final ideal image.

295 Step 1: channel processing. Cut the initial image into three channels: R, G and B, and each  
296 channel can get its own information. The formula is as follows:

$$297 Y_i = \text{image}(Y_i) \quad (i = R, G, B) \quad (22)$$

298 In equation (22),  $i$  represents three channels of R, G, and B, and  $Y$  represents the original  
299 image of CNN.

300 Step 2: CNN training. The formula is as follows:

$$301 Y_i = \max(0, S_i * Y_{i(i-1)} + C_i) \quad (i = 1, 2, 3) \quad (23)$$

302 In equation (23),  $S_i$  represents the convolution kernel of each layer of the CNN,  $C_i$  represents  
303 the bias of each layer of the CNN, and  $Y_{i(i-1)}$  represents the output result after the fifth  
304 convolution.

305 Step 3: Image fusion. The formula is as follows:

$$306 Y = \text{cat}(Y_R, Y_G, Y_B) \quad (24)$$

307 Step 4: NSCT algorithm processing. The NSCT operation is performed on the fused image.  
308 This method uses a tower decomposition algorithm to decompose the initial image into two parts,  
309 high-pass and low-pass. Then use NSDFB (Non-Subsampled Directional Filter Banks) to  
310 decompose the high frequency sub-band into several directional sub-bands, and for the low  
311 frequency part, continue to de-compose according to the method described above. The final image  
312 is obtained.

313 By using deep learning convolutional neural network and NSCT technology to enhance the  
314 color, the ideal goal has been achieved. NSCT can achieve rapid trans-formation at different scales  
315 and directions. The experiment proves that the method combining SRCNN and NSCT can not only  
316 further enhance the degree of idealization of color, but also maintain and enhance the edge details  
317 of the image to the greatest extent.

318 As mentioned above, the method of adaptive exposure graph is used to deal with the exposure  
319 problem, and the color and edge details are enhanced by combining SRCNN and NSCT technology,  
320 which plays an irreplaceable role in improving the image clarity, enhancing the color and edge  
321 details.

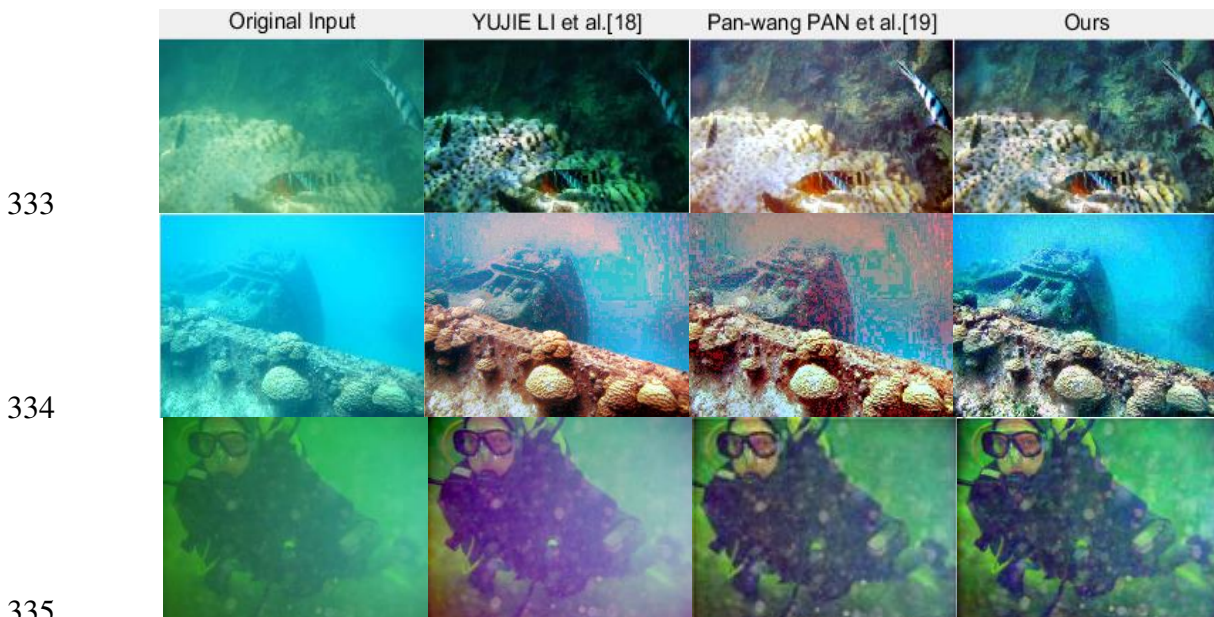
## 322 4. Experimental Results

323 The method proposed in this paper systematically illustrates how to transform an underwater  
324 image full of noise, underwater fog and dim light into a high-quality image that can be clearly read  
325 by people from two aspects of image restoration and enhancement. Among them, it is better than  
326 other methods in defogging underwater under-exposure images, enhancing image color,  
327 maintaining and enhancing local edge details.

### 328 4.1. Experimental result and theoretical analysis

329 In order to further verify the superiority of the method used in this paper, this paper compares  
 330 the methods of other literatures in the image restoration and image enhancement stages, as follows:

331 The first stage. This paper compares the method of YUJIE LI et al. [18] and the method of  
 332 Pan-wang PAN et al. [19], and the results are shown in Fig.5.



335 **Fig.5.** Comparison of the results of different image restoration methods

336 It can be clearly seen from the comparison of the three sets of images in Fig. 5 that the literature  
 337 [18] is relatively good in defogging and maintaining details of the image, but the color of the local  
 338 area is darker, and the color difference from the normal image is too large. And a certain blur  
 339 appears in the image after denoising. Literature [19] is relatively good at defogging and color  
 340 control, but there is also a certain degree of blurring in the image, and it does not make much  
 341 contribution to the retention of edge details, resulting in the desalted detail texture of the processed  
 342 image and the lack of clarity. The method used in this paper is better than other methods in  
 343 denoising, fogging, preserving details and protecting colors of underwater under-exposed images.  
 344 In order to further illustrate the clarity comparison of different methods, signal to noise ratio (SNR)  
 345 is adopted, as shown in table 1.

346

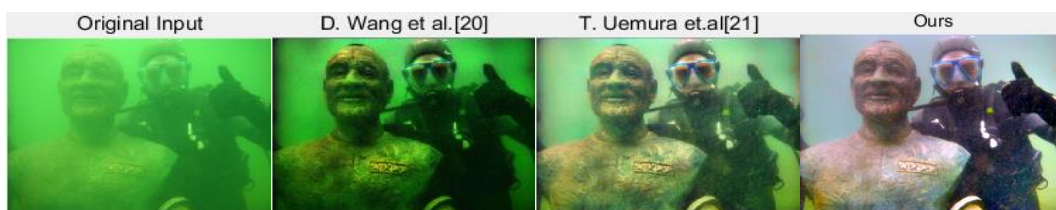
**Table 1** SNR comparison

No.	References [18]	References [19]	Ours
Fig.4(a)	36.46	37.52	40.67
Fig.4(b)	38.61	39.27	42.39
Fig.4(c)	36.53	37.14	40.13

347

348 The second stage. The method in this paper will be compared with the method proposed by D.  
 349 Wang et al. [20] and T. Uemura et al. [21]. The qualitative comparison is shown in Fig.6.

350



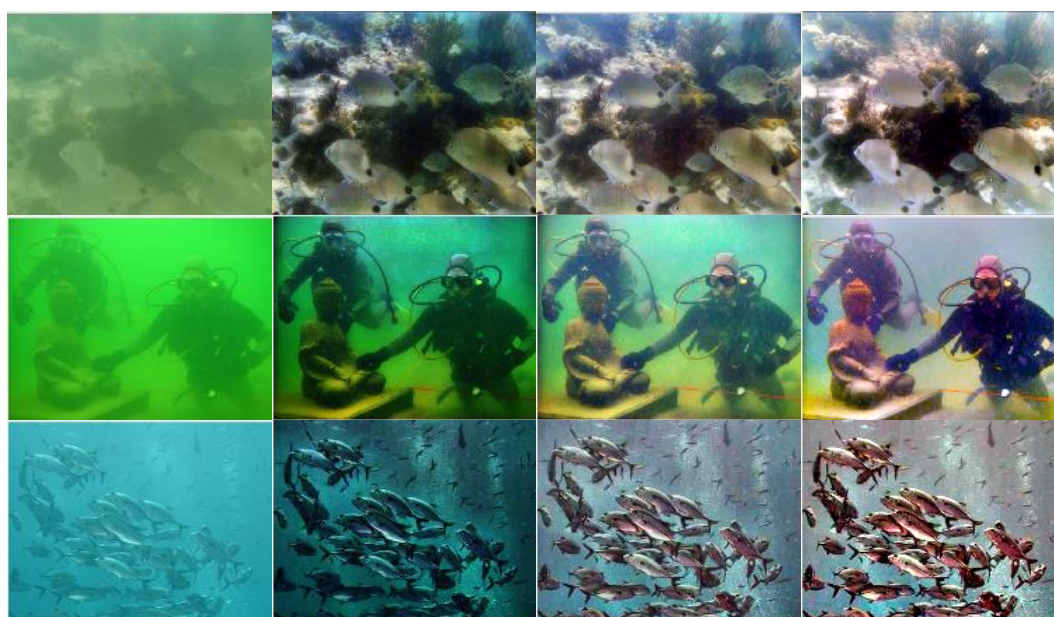


Fig. 6. Comparison of the results of different image enhancement methods

From left to right, the four sets of images in Fig.6 are the original image, D. Wang et al. [20], T. Uemura et al. [21], and the method of this paper. It can be seen that the results achieved by D. Wang et al.'S method can achieve a dehazing effect, but the image clarity and color have not achieved the desired effect. Although the method of T. Uemura et al. Has achieved the effect of defogging, and can make a certain degree of effort in terms of color preservation and enhancement, it fails to improve the degradation of edge details. However, the method in this paper not only fully realizes the efficient defogging effect, but also enhances the image color and edge texture, making the image sharper and achieving the ideal visual effect.

Next, the paper uses the image Entropy and gradient average value(AVG) to calculate and analyze the corresponding implementation results of different methods in Fig.6, as shown in Table 2. Among them, the entropy of the image can be used to represent the statistical characteristics of the image. It shows the average signal amount. The size of the entropy value intuitively highlights the quality and clarity of an image. The gradient average value can not only reflect the sharpness of the image, but also can indicate changes in edge texture details. As the gradient average value becomes larger, the blurriness of the image will become smaller, that is, the more the image will be the clearer.

Table 2 Comparison of entropy and AVG

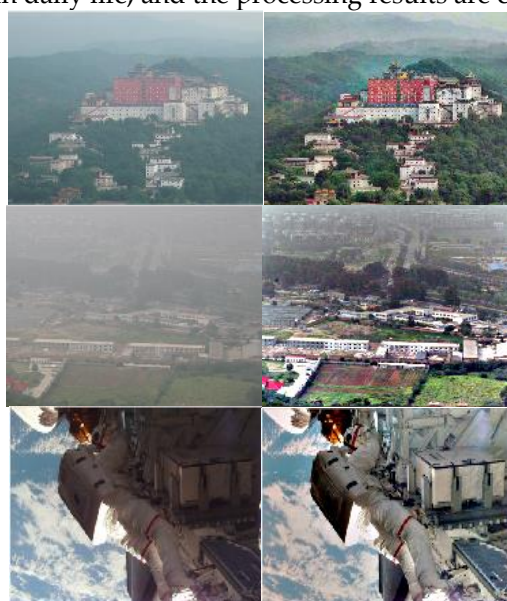
Image	Method	Entropy	AVG
Image1	D.Wang	7.4218	0.1179
	T.Uemura	7.6126	0.1258
	Our	7.7829	0.1324
Image2	D. Wang	7.3852	0.1098
	T.Uemura	7.4635	0.1175
	Our	7.5397	0.1253
Image3	D. Wang	7.3758	0.1137
	T.Uemura	7.5461	0.1248
	Our	7.6283	0.1309
Image4	D. Wang	7.4106	0.1135
	T.Uemura	7.4913	0.1268
	Our	7.5372	0.1325

It is obvious from the image entropy and gradient average values in Table 2 that the method used in this paper is better than the other two methods. Experiments show that the method used in

374 this paper is very effective in solving the problems of noise, fog, dim light, color degradation and  
 375 loss of edge details in underwater images. Therefore, it is known from experiments and qualitative  
 376 analysis that the method used in this paper is superior to the other two methods, and further  
 377 improves the visual effect of underwater images.

#### 378 4.2. Application under other circumstances

379 The experimental verification shows that the method in this paper also plays a certain role in  
 380 restoring and enhancing non-underwater images. It can also deal with foggy and noisy  
 381 underexposure images taken in daily life, and the processing results are considerable. See Fig.7.



(a) original image (b) processed image

Fig.7. Processing effect of underexposure in other cases

387 This section may be divided by subheadings. It should provide a concise and precise  
 388 description of the experimental results, their interpretation as well as the experimental conclusions  
 389 that can be drawn.

#### 390 5. Discussion

391 In the first stage of this paper (section 4.1), the restoration of underwater under-exposure  
 392 images is carried out, including two experiments of underwater image de-noising and de-fogging.  
 393 The specific implementation method and experimental results are shown in sections 2.1 and 2.2. An  
 394 improved wavelet threshold function is used for denoising, in which the Bayesian threshold is used,  
 395 and the threshold of each layer can be adaptively reduced as the wavelet decomposition scale  
 396 increases, and it is also used in [10] Particle swarm optimization algorithm, its benefits are that the  
 397 algorithm is simple and easy to implement, the convergence speed is fast, and fewer parameters are  
 398 set; Use the method of MSRRCR combined with the guide filter to remove fog. Among them, MSRRCR  
 399 can not only remove the fog, but also can greatly protect the color of the image during the  
 400 processing. The restoration effect of the image is remarkable, and the efficiency of the algorithm is  
 401 improved. In Fig. 5, the experimental results of this paper are compared with YUJIE LI et al. [18]  
 402 and the method of Pan-wang PAN et al. [19]. YUJIE LI et al. [18] first performed defogging and  
 403 gamma correction on the original image, then SRCNN is used to enhance the color of the image, the  
 404 contribution of this paper is that the color of the image is well protected and enhanced, the  
 405 disadvantage is that the enhancement of the edge details of the image has not achieved the desired  
 406 effect, and the brightness processing also did not achieve good results. Pan-wang PAN et al. [19]  
 407 first adopted a multi-scale iterative framework to remove underwater scattering, then refined it  
 408 through an adaptive bilateral filter, and finally used NSCT to perform edge denoising. The

409 advantage of this paper is the use of deep learning methods to remove the color distortion of the  
 410 image, the disadvantage is that there are no targeted measures for underwater fog, which results in  
 411 the processed image is not very clear. From the experimental results and the signal-to-noise ratio of  
 412 the image, it can be seen that the method of restoration and enhancement of underwater  
 413 underexposure images with preservation of details used in this paper is optimal.

414 The second stage (Section 4.2) of this paper is to enhance the underwater image, including the  
 415 exposure processing of the underwater image, the enhancement of image color and edge details, the  
 416 method of adaptive exposure map combined with a guided filter is adopted. After the first stage,  
 417 the overall effect of the image is dark, although after the improved histogram equalization process,  
 418 there is still a certain degree of poor exposure for the local area of the image, so the method of  
 419 solving the optimal value of the adaptive exposure map combined with the guided filter method  
 420 perfectly solves this problem. Finally, for the phenomenon that the processed underwater image  
 421 may not have obvious local area colors and lost edge details, this paper uses the method of SRCNN  
 422 combined with NSCT, which has the best effect on enhancing the local color and edge texture. In  
 423 comparison experiments with D. Wang et al. [20] and T. Uemura et al. [21], it can be concluded that  
 424 there are different degrees of shadows in their implementation effects, and the sharpness and  
 425 saturation of colors in the images is not as effective as the method of this paper. Further, by  
 426 comparing the experimental results with those in Table 2, we can see that the method used in this  
 427 paper is the best.

## 428 6. Conclusions

429 To solve the problem of underwater underexposure image restoration and enhancement, this  
 430 paper adopts the method of image preprocessing and SRCNN. First, the improved wavelet  
 431 threshold function was used to solve the image noise problem, and then the MSRCR combined  
 432 guided filter was proposed to remove the underwater fog. Experiments show that the effect of  
 433 defogging is better than the existing methods, and the efficiency of calculation is higher, which is  
 434 also a great innovation of this paper. Then, the improved histogram equalization is used to improve  
 435 the brightness of the image and play a role in enhancing the color of the image. Finally, SRCNN  
 436 algorithm combined with NSCT technology is used to further improve the phenomenon of local area  
 437 edge detail dilution and color degradation in the image after exposure processing. The experimental  
 438 results show that the underwater underexposure image restoration and enhancement method is  
 439 better than other methods and achieves the desired goal. However, there are still some shortcomings  
 440 in the method in this paper. For underwater images with heavy noise, too much fog and too little  
 441 light, the advantages are not obvious after image processing. Next, it will make further  
 442 consummation in this respect.

## 443 List of abbreviations

Abbreviations	Meaning
SRCNN	Super-resolution convolutional neural network
MSRCR	Multi-scale retinex with color restoration
NSCT	Non-subsampled contour transform
AVG	Gradient average value
MSR	Multi-Scale Retinex
SNR	Signal to noise ratio
CNN	Convolutional Neural Networks
NSDFB	Non-Subsampled Directional Filter Banks

## 444 Acknowledgements

445 Thanks to my teachers and classmates for their help in the paper writing; It was with their  
 446 encouragement and guidance that I finally finished this paper.

#### 447 **Authors' contributions**

448 The first draft of the paper, Formula analysis, review of articles and experimental data are  
 449 completed by Ke Liu, Revision, review and fund management of papers are completed by Xujian  
 450 Li.

#### 451 **Authors' information**

452 Xujian Li, Associate professor, master tutor, he is currently working at the school of computer  
 453 science, shandong university of science and technology, Qingdao, Shandong, China. Main research  
 454 areas: graphics and image processing, computer vision, cloud computing.

455 Ke Liu, Master degree, he is currently studying at the school of computer science, shandong  
 456 university of science and technology, Qingdao, Shandong, China. Main research areas: graphic  
 457 image processing, deep learning.

#### 458 **Funding**

459 The authors acknowledge this paper was supported by the National Key Research and  
 460 Development Program of China under Grant 2017YFC0804406.

#### 461 **Availability of data and materials**

462 Data and implementation codes for all experiments are based on python and matlab.

#### 463 **Competing interests**

464 Not applicable

#### 465 **Author details**

466 <sup>1</sup> Associate professor, master tutor, member of jiusan society, Shandong university of science and  
 467 technology, 266000; xjlee@163.com. Tel: +86-13863963003

468 <sup>2,\*</sup> Master, school of computer science and engineering, Shandong university of science and  
 469 technology, 266000; [keliucs@163.com](mailto:keliucs@163.com). Tel: +86-18354238263

#### 470 **References**

- 471 1. S. Li and X. Kang, "Fast multi-exposure image fusion with median filter and recursive filter," IEEE Trans.  
 472 Consum. Electron. May 2012, vol. 58, no. 2, pp. 626–632.
- 473 2. J. Im, J. Jeon, M. H. Hayes, and J. Paik, "Single image-based ghostfree high dynamic range imaging using  
 474 local histogram stretching and spatially-adaptive denoising," IEEE Trans. Consum. Electron. Nov. 2011,  
 475 vol. 57, no. 4, pp. 1478–1484.
- 476 3. M. Bertalmío and S. Levine, "Variational approach for the fusion of exposure bracketed pairs," IEEE  
 477 Trans. Image Process. Feb. 2013, vol. 22, no. 2, pp. 712–723.
- 478 4. A. Galdran z, D. Pardo, A. Picon, and A. Alvarez-Gila, "'Automatic red-channel underwater image  
 479 restoration," Journal of Visual Communication and Image Representation. 2015 , vol. 26, pp. 132–145,.
- 480 5. A. S. A. Ghani and N. A. M. Isa, "Underwater image quality enhancement through integrated color model  
 481 with rayleigh distribution," Applied Soft Computing, 2015, vol. 27, pp. 219–230.
- 482 6. C. Li and J. Guo, "Underwater image enhancement by dehazing and color correction," Journal of  
 483 Electronic Imaging, 2015, vol. 24, pp. 033023–033023.
- 484 7. Chongyi Li1, Jichang Guo1, Yanwei Pang1, Shanji Chen2, Jian Wang." SINGLE UNDERWATER IMAGE  
 485 RESTORATION BY BLUE-GREEN CHANNELS DEHAZING AND RED CHANNEL CORRECTION",  
 486 2016 IEEE International Conference on Acoustics, Speech and Signal Processing (ICASSP). 20-25 March  
 487 2016.
- 488 8. Shiguang Liu, Yu Zhang. Detail-Preserving Under-exposure Image Enhancement via Optimal Weighted  
 489 Multi-Exposure Fusion[J]. IEEE Transactions on Consumer Electronics, Aug. 2019, vol. 65, no. 3, 303 – 311.
- 490 9. Israt Zahan Nishu ; Muhammad Fuad Tanjim ; A. S. M. Badrudduza ; Md. Al Mamun. A New Image  
 491 Despeckling Method by SRAD Filter and Wavelet Transform Using Bayesian Threshold[C]. 2019  
 492 International Conference on Electrical, Computer and Communication Engineering (ECCE), 7-9 Feb. 2019.

- 493 10. Tang peng, guo baoping. Wavelet de-noising analysis of improved threshold function optimization  
494 method [J]. Signal processing. 2017, 33(1).102-110.
- 495 11. Yuhong Liu ; Hongmei Yan ; Shaobing Gao ; Kaifu Yang. Criteria to evaluate the fidelity of image  
496 enhancement by MSRCR[J]. IET Image Processing. May 2018, vol.12,no,6.
- 497 12. Dong lili, ding chang, xu wenhai. Two improved methods for image enhancement based on histogram  
498 equalization [J]. Chinese Journal of Electronics, 2018.10: 2367-2375.
- 499 13. K. Tang, J. Yang, and J. Wang, "Investigating hazerelevant features in a learning framework for image  
500 dehazing," in Computer Vision and Pattern Recognition,2014 IEEE Conference on. IEEE, 2014, pp. 2995-  
501 3002.
- 502 14. Nahla M. H. Elsaid ; Yu-Chien Wu. Super-Resolution Diffusion Tensor Imaging using SRCNN: A  
503 Feasibility Study\*[C]. 2019 41st Annual International Conference of the IEEE Engineering in Medicine and  
504 Biology Society (EMBC),July 2019.
- 505 15. Yongpeng Dai ; Tian Jin ; Yongping Song ; Hao Du ; Dizhi Zhao. SRCNN-Based Enhanced Imaging for  
506 Low Frequency Radar[C]. 2018 Progress in Electromagnetics Research Symposium (PIERS-Toyama),1-4  
507 Aug 2018.
- 508 16. Zhishe Wang; Jiawei Xu; Xiaolin Jiang; Xiaomei Yan. Infrared and visible image fusion via hybrid  
509 decomposition of NSCT and morphological sequential toggle operator[C]. Optik.2019.12.
- 510 17. Liu Jiahuan ; Zhang Jian ; Du Yunfei. A Fusion Method of Multi-spectral Image and Panchromatic Image  
511 Based on NSCT Transform and Adaptive Gamma Correction[C]. 2018 3rd International Conference on  
512 Information Systems Engineering (ICISE), 4-6 May 2018.
- 513 18. YUJIE LI , CHUNYAN MA, TINGTING ZHANG, JIANRU LI,ZONGYUAN GE, YUN LI, AND SEIICHI  
514 SERIKAWA. Underwater Image High Definition Display Using the Multilayer Perceptron and Color  
515 Feature-Based SRCNN[J]. IEEE Access. ENVIRONMENTS. June 2019, vol.7.
- 516 19. Pan-wang PAN, Fei YUAN, En CHENG. De-scattering and edge-enhancement algorithms for underwater  
517 image restoration[J]. Frontiers of Information Technology & Electronic Engineering, 2019, Vol.20 (6),  
518 pp.862-871.
- 519 20. H. Lu, D. Wang, Y. Li, J. Li, X. Li, H. Kim, S. Serikawa, and I. Humar,"CONet: A cognitive ocean network,"  
520 IEEE Wireless Commun. to be published. July.2019, vol.26,no.3,90-96.
- 521 21. H. Lu, Y. Li, T. Uemura, H. Kim, and S. Serikawa, "Low illumination underwater light field images  
522 reconstruction using deep convolutional neural networks," Future Gener. Comput. Syst. May 2018, vol.  
523 82, pp. 142-148.

524

# Figures

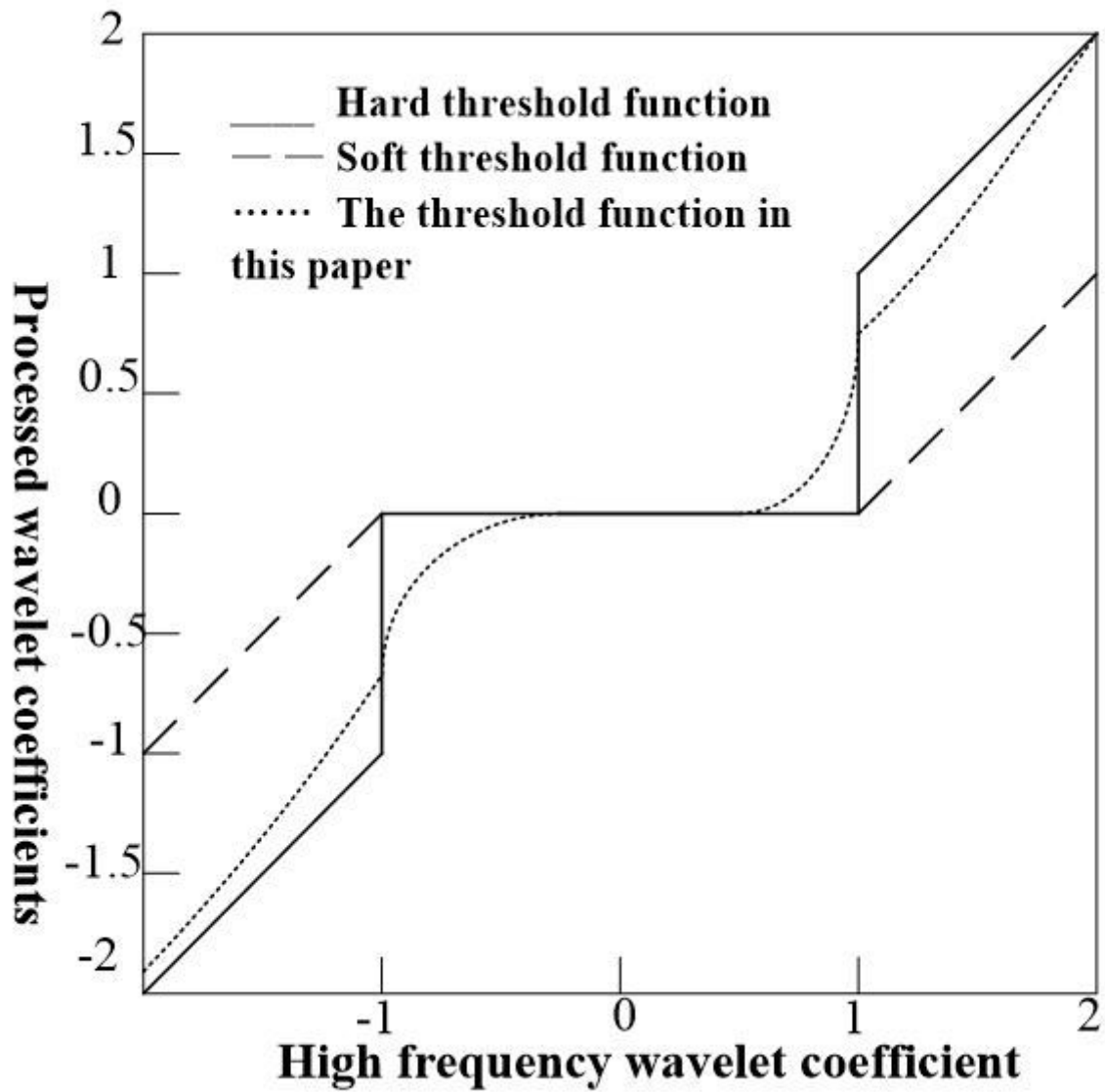


Figure 1

Comparison of different threshold function curves



(a) Original image    (b) Denoised image

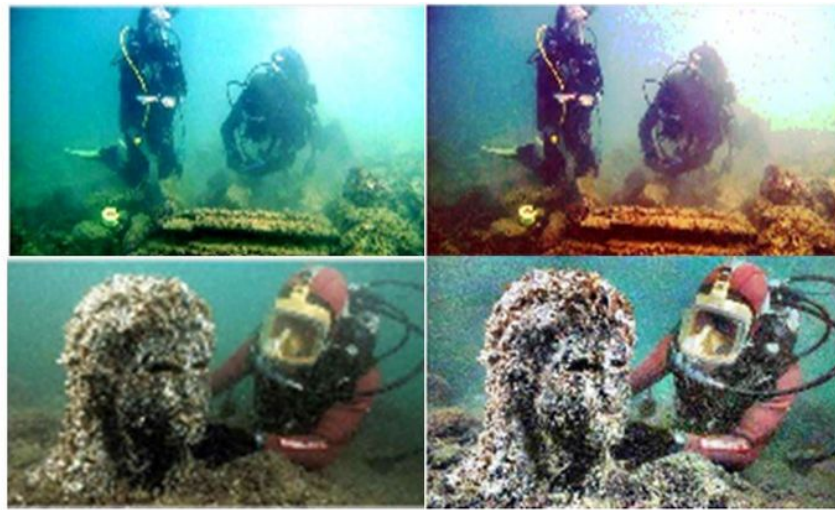
Figure 2

Denoising results



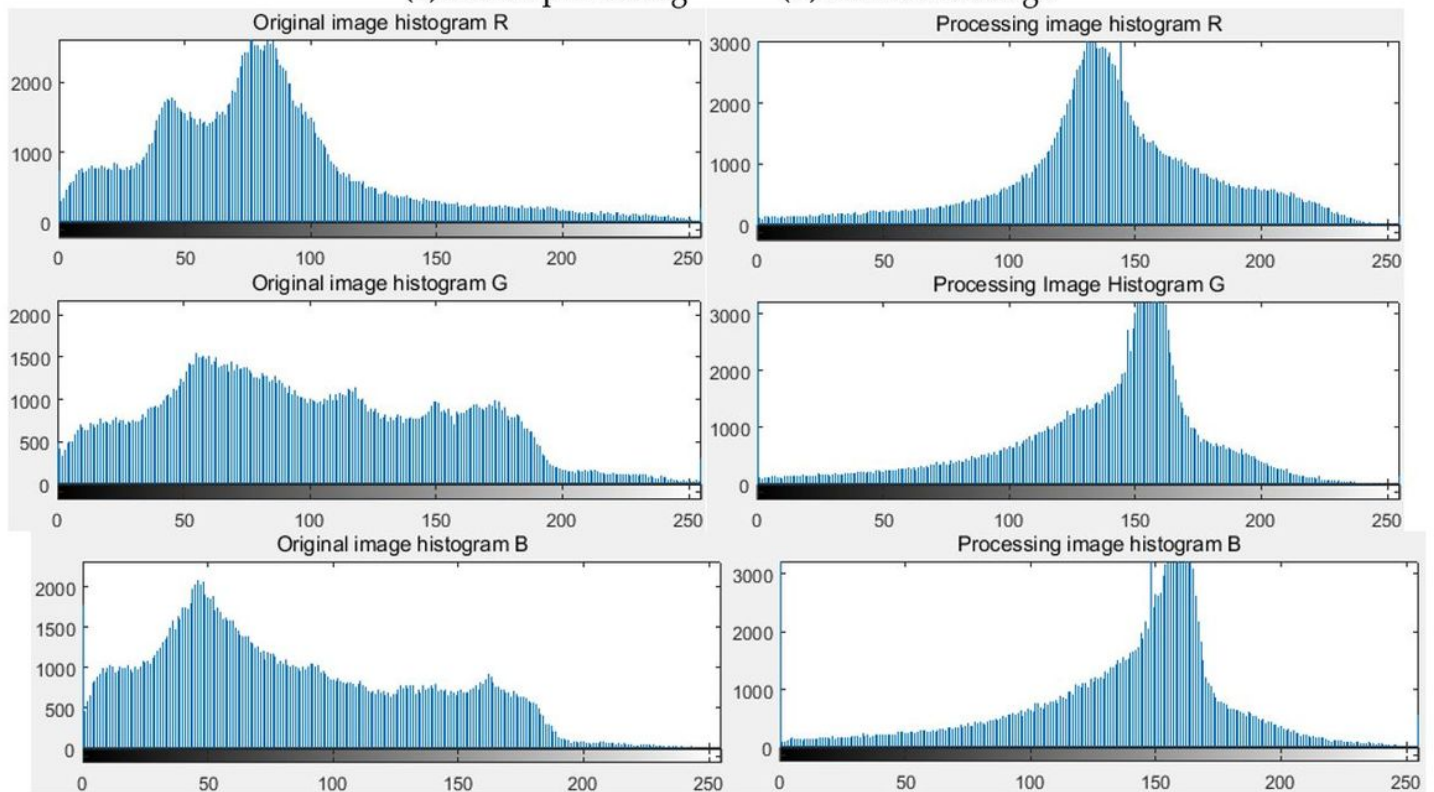
Figure 3

Dehazing effect (the original image on the left; the image after the defogging on the right).



(a) Before processing

(b) Processed image



(c) Is the histogram of the second image in (a)

Figure 4

Improved histogram equalization results

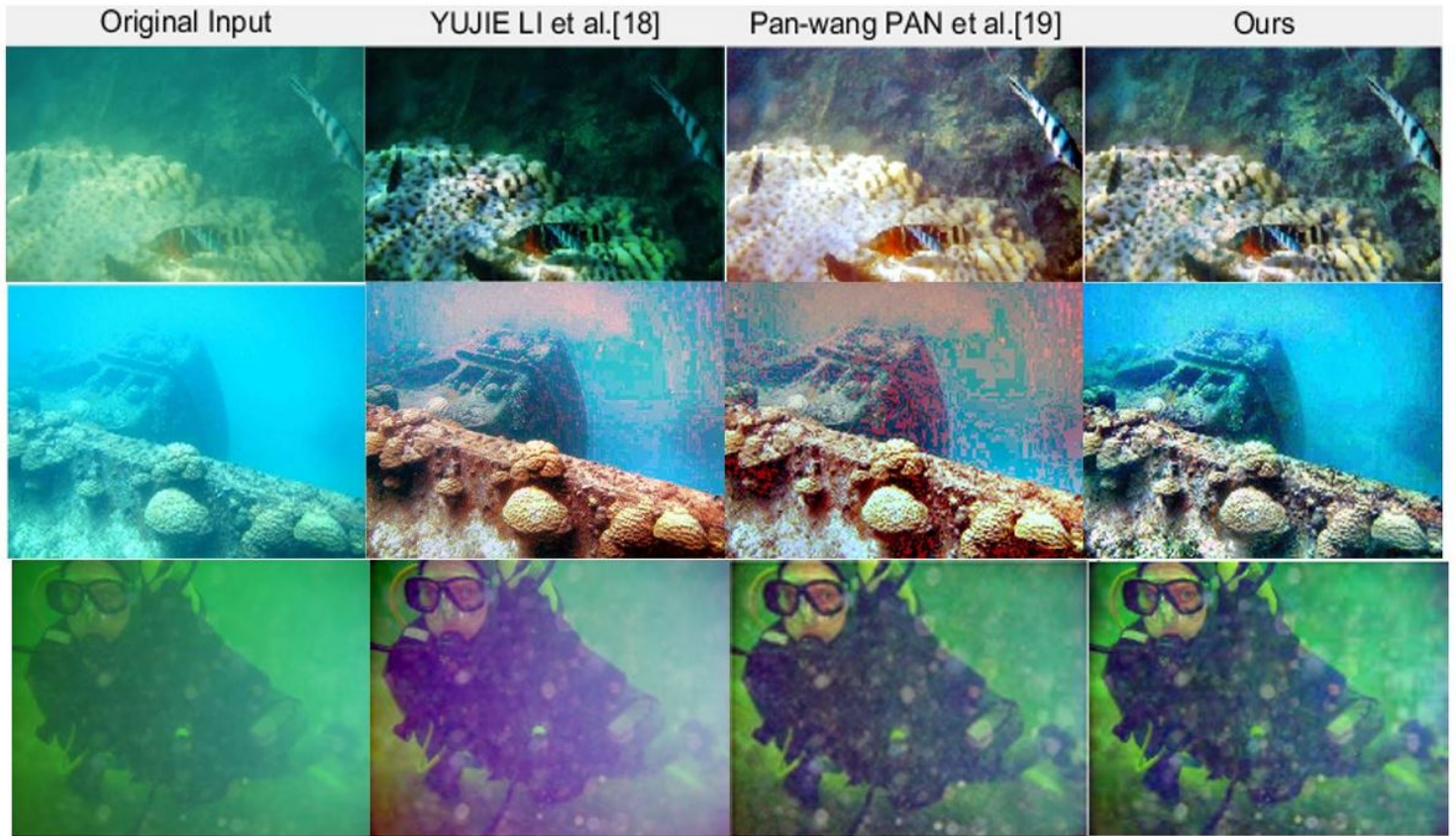


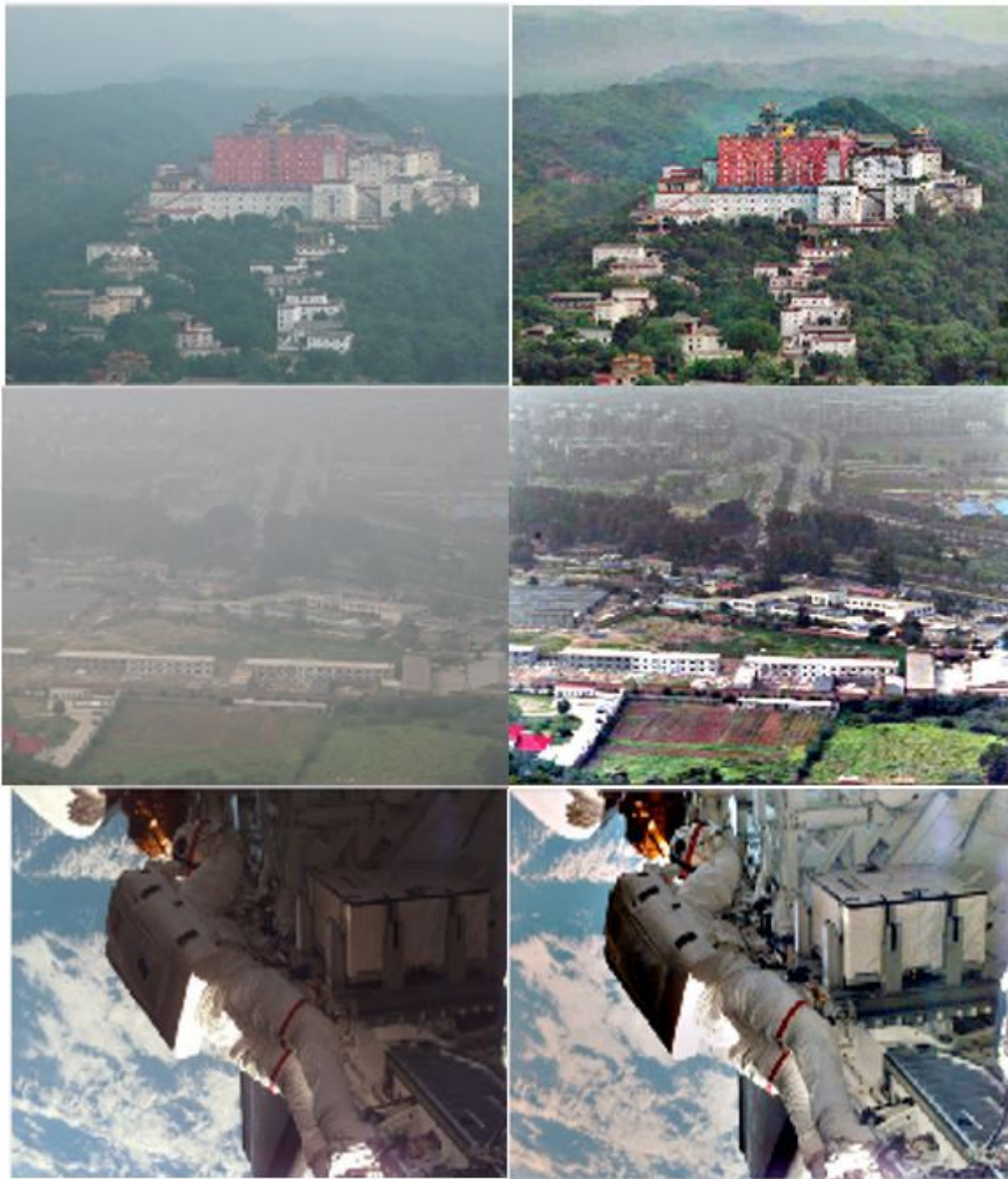
Figure 5

Comparison of the results of different image restoration methods



Figure 6

Comparison of the results of different image enhancement methods



**(a)** original image      **(b)** processed image

Figure 7

Processing effect of underexposure in other cases